

Generation and suppression of runaway electrons in ASDEX Upgrade disruptions

G. Pautasso, P.J. McCarthy (*), C. Fuchs, R. Dux, S. Potzel, G. Papp, M. Sertoli, G. Tardini, K. Lackner, A. Scarabosio, A. Mlynek, L. Giannone, the ASDEX Upgrade team the EUROfusion MST team (+),

Max-Planck-Institut für Plasmaphysik, 85748 Garching, Germany,

(*) Department of Physics, University College Cork, Cork, Ireland, (+) <http://www.euro-fusionscipub.org/mst1>

Introduction

Runaway electrons (REs) are expected to be generated in ITER disruptions at any significant plasma current. While the generation mechanisms of REs are believed to be understood, there is not a general consensus on which loss mechanisms are dominant in present experiments, and which one will prevail in ITER. This makes the calculation of the expected RE current and energy - and the consequent damage to the plasma facing components - uncertain and the design of the ITER disruption mitigation system challenging.

ASDEX Upgrade (AUG) disruptions, typically of diverted and elongated plasmas, do not exhibit formation of RE beams for the following reasons: Usually, a disrupting plasma has a density large enough to suppress the Dreicer generation; the avalanche generation is not expected to be significant in AUG; during the current quench, an elongated plasma becomes vertically unstable, moves up- or downwards, becomes limited on the lower or upper divertor and develops a halo, i.e. a region of open flux surfaces from which the REs escape, within milliseconds. Therefore, in order to allow studies of RE generation and dissipation during disruptions, a scenario for RE generation during the thermal quench had to be - and was - established during the 2014 campaign.

This paper presents the analysis and results of a series of RE-dedicated discharges. The magnetic equilibrium and the free-electron density profile reconstruction, the evaluation of the argon concentration during the whole RE beam, which allow the comparison between measured and computed friction force on the REs, are the main results of the work presented in the following.

Experimental scenario and measurements

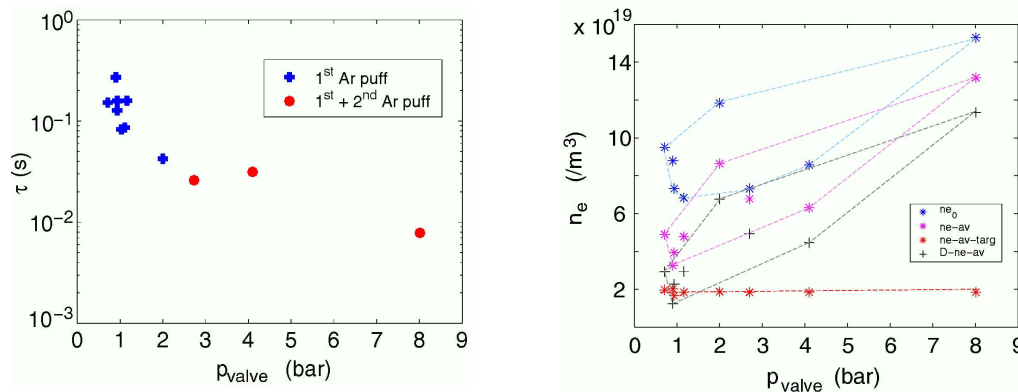
RE generation. REs have been generated by injecting between 0.07 and 0.2 bar×litre of argon in a low target density (volume averaged $n_e \leq 2 \times 10^{19} \text{ m}^{-3}$) circular plasma, with a current of 0.8 MA, a toroidal magnetic field of 2 T and 2 MW of ECRH heating. The injected argon induces a fast quench of the current carried by thermal electrons, followed by a long-lived runaway beam, forming a toroidal current of up to 300 kA, and lasting up to 380 ms. Although the target plasmas were similar (repeats), different initial RE current were observed, independently of the amount of argon injected – for reasons not yet identified.

RE suppression. In some of the RE beams generated, argon was injected a second time (0.17 and 0.7 bar×litre with a second valve) with a delay of 70 ms from the first argon puff. The RE current decay rates, after both the first and the second argon puff, show a clear dependence on the argon amount injected – i.e. the more gas the faster the decay, as illustrated by fig. 1 - suggesting that RE energy loss by collision (friction and radiation induced) with the electrons and the high Z impurity atoms is a significant RE dissipation mechanism. In the following section, the expected – from density measurements – and observed collisional damping are discussed.

Gas inventory. The amount of deuterium gas puffed into the vessel to fuel the plasmas under analysis, integrated over the whole discharge, ranges between 3×10^{20} and 8×10^{20} atoms. The amount of argon injected into the vessel and plasma, within a few ms after the opening of the fast valve, amounts to 2.4×10^{21} argon atoms per bar originally in the valve reservoir. Since the valve reservoir pressure was varied between 0.7 and 7 bar (and the 7 bar injection followed a 1 bar), a total amount between

1.7×10^{21} and 1.9×10^{22} argon atoms was injected into the vessel in a single discharge. A uniform distribution of these argon amounts within an empty vessel volume of 39.7 m^3 would result in neutral densities ranging between 4.3×10^{19} and $4.8 \times 10^{20} \text{ m}^{-3}$. The ratio of the argon versus deuterium amount injected varies from 2 to 65.

The maximum vessel pressure, measured by two Baratron capacitance manometers (absolutely calibrated but too slow to measure the time evolution of the pressure) are in agreement with the total amount of injected gas. The fast pressure gauges were unfortunately saturated during the RE beam.



Left: fig. 1. Decay time, $\tau = I_p/(dI_p/dt) \sim \langle I_p \rangle / (\Delta I_p / \Delta t)$ of the RE current versus argon pressure in the valve.

Right: fig. 2. Central (n_{e0}) and volume averaged electron (n_{e-av}) density after argon injection; volume averaged electron density in target plasma and increase ($D-n_{e-av}$) of the density after argon injection.

Electron density. Line integrated measurements of the electron density, n_e , are available during the whole RE beam lifetime from 5 DCN chords and from 2 CO₂ chords. The n_e profiles could be reconstructed for all the discharges during most of the RE beam because the magnetic equilibria could be calculated. The first and second argon injection increase significantly the volume averaged n_e : Fig. 2 reports an increase of a factor between 2 and 6 calculated from density measurements recorded 25 ms after the first argon puff ($p_{\text{valve}} < 2.5$ bar) and 10 ms after the second argon puff ($p_{\text{valve}} > 2.5$ bar).

Plasma position and its control. The circular plasma is vertically stable; the position and the shape of the plasma are in agreement with Soft X-Ray profiles. The plasma control system does not contribute to the vertical stability because the current in the control coils is part or all of the time saturated. A slow vertical displacement sets-in only in a few cases and does not affect the overall current decay rate of the RE beam.

Current control. The plasma current is ramped down by the control system; after injection of “small” amounts of argon, the controlled current follows the pre-programmed time trace; larger amounts of argon increase the RE losses, accelerate the current decay and the OH system cannot keep the actual current at the level of the reference value.

Current decay. The RE current does not exhibit a regular monotonic decay but rather a “bumpy” time behaviour correlated to sporadic MHD events, which are under investigation. The final phase of the current is often characterized by a faster loss of 30–100 kA, followed again by the slower decay of some tens of kA. Alternatively the current goes to zero with a constant slope.

The value of the edge safety factor (q_{edge}) at the time of the rapid current drop is not known in general, because the equilibrium reconstruction fails and radiation emission from the beam is not strong enough to allow its localization. Linear time extrapolation of q_{edge} , toward the end of the RE beam, indicates that its value will not drop below 5 at the time of the final current decay.

Radiated power. The foil bolometers measure a total radiated energy of the order of magnitude of the initial kinetic and magnetic energy of the RE beam. This suggests that radiation plays a significant role in the RE energy dissipation. Measurements of Bremsstrahlung and synchrotron radiation are not

available for this dedicated experiment.

HXR spectrum. Time-resolved measurements of gamma spectra from a gamma/neutron spectrometer are available and can give indication of the RE energy spectra, if interpreted with a model of RE-matter interaction. The spectrometer line of view crosses the beam on the midplane and intersects the inner wall, where the RE beam is limited and slowly scraped off. Therefore most of the photons should be generated by the interaction of the REs with the wall material. The gamma spectrum is peaked at energies of ~ 100 keV and does not change its form significantly as the RE current decays.

RE collisional damping

REs lose energy through different known mechanisms: By inelastic collision mainly with bound and free electrons, through small angle scattering and transfer of energy to the matter in which they travel; by collision with ions and Bremsstrahlung radiation; by cyclotron and synchrotron radiation. The first mechanisms, i.e. the friction force of the electrons on the REs, is discussed in this contribution, since the other mechanisms are evaluated to be smaller.

The RE current time evolution (with time constant τ_r) is expected to be described by

$$1/\tau_r = dn_r/dt \quad 1/n_r \simeq e(E_\phi - E_c)/p_r \quad \text{Eq. (1)}$$

where E_ϕ is the toroidal electric field, E_c is the so-called critical electric field, n_r is the RE density and “ p_r ” is the average RE momentum.

Electric field. The evaluation of E_ϕ in the plasma requires a self consistent modelling of the plasma current evolution, which is mainly carried by the REs in the analysed discharges. Numerical modelling has not been carried out yet and therefore E_ϕ is not precisely known. Nevertheless, measurements of the loop voltage (U_{loop}) at different poloidal positions around the plasma are available. The closest – to the plasma – U_{loop} coil is inside the vessel, behind the inboard shield, some 10 cm far from the plasma surface; the measurement from this coil is equipped with a 30 Hz low-pass filter, which limits the validity of the measurements to slow transients (RE plateau). Faster measurements (30 kHz bandwidth) are available under the lower divertor and on the LFS, further away from plasma. The values of the poloidal flux from equilibrium reconstruction are also available and, in principle, allow the calculation of the electric field at the plasma surface. In reality, since this calculation requires the time derivative of the separatrix-coil flux difference, the resultant E_ϕ is very noisy.

An average E_ϕ can also be calculated knowing the plasma self-inductance and the mutual-inductance between the plasma and other coils/structures:

$$2\pi R_c E_\phi \simeq L_p dI_p/dt + M_{\text{OH-p}} dI_{\text{OH}}/dt + M_{\text{vv-p}} dI_{\text{vv}}/dt \quad \text{Eq. (2)}$$

where $M_{\text{OH-p}}$ and $M_{\text{vv-p}}$ are the mutual inductances between the OH coils and the plasma, and between the vessel structures and the plasma, respectively.

The fast and slow U_{loop} measurements and the estimations with Eq. (2) give the following consistent picture:

- during the CQ, transient loop voltages of 40-50 V are reached;
- during the RE plateau, the loop voltage decreases from 10 to a few V in all cases;
- during the fast RE termination caused by the second argon injection, transient loop voltages up to 10 V are generated.

$E_\phi = U_{\text{loop}} / (2\pi R_c) \sim U_{\text{loop}} / 10$, since the current major radius, $R_c \sim 1.6$ m.

The critical electric field. E_c is a linear function of the free and bound electron density; therefore its estimation requires knowledge of the plasma atomic species and their ionization state:

$$E_c = e^3 n_e \ln(\Lambda_{e,\text{free}}) / (4\pi \epsilon^2 m_e c^2), \quad n_e = n_{e,\text{free}} + \ln(\Lambda_{e,\text{bound}})/\ln(\Lambda_{e,\text{free}}) n_{e,\text{bound}} \quad \text{Eq. (3)}$$

Impurities other than argon are neglected here. Fig. 3 shows E_c as function of single-ionized argon

density.

Argon concentration. A total of 25 + 17 line integrated measurements of light emitted by Ar⁺ at 401.39 nm are available during the RE beam lifetime with a high time resolution. They allow a spatially resolved calculation of the Ar⁺ density, when the electron temperature and density are known, since the line radiance is given by the following integral along the line of sight:

$$L = 1/4\pi \int n_e n_{Ar} 0.343 f_1 X_{eff}(T_e, n_e) dl \quad \text{Eq. (4)}$$

The photon emissivity coefficient X_{eff} for the Ar⁺ transition $3p^4(3P)4p \ ^4D_{7/2} \rightarrow 3p^4(3P)3d \ ^4D_{7/2}$ at 401.39 nm has been calculated from a collisional radiative model. The model does only consider the population of the upper states by electron excitation collisions. For the solution of the collisional radiative model, the ADAS208-code has been used. It gives the photon emission rate density per Ar⁺ ion density and electron density for the whole multiplet. Within the multiplet, the specific line has a relative line strength of 0.343 when assuming LS-Coupling. The Ar⁺ fractional abundance f_1 has been calculated from the ADAS data sets for rate coefficients of ionisation and recombination assuming a balance of ionisation and recombination rates; $(f_1 X_{eff})$ has a maximum at $T_e = 2.4$ eV.

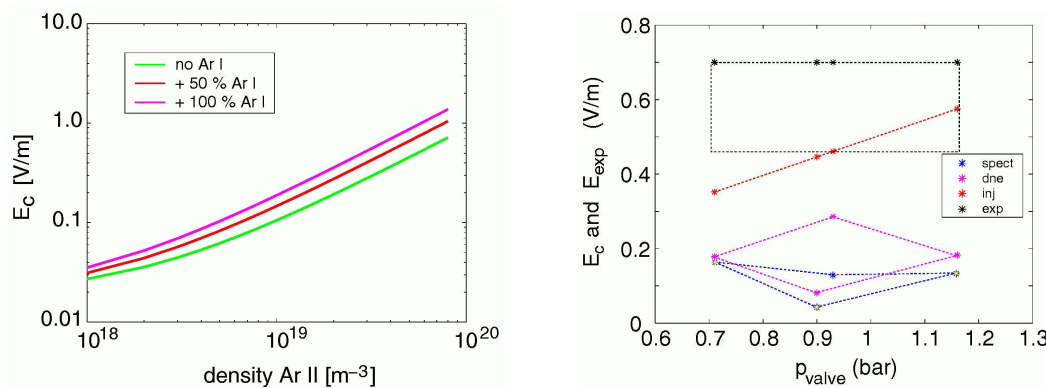
The argon concentration in the target plasma, calculated with Eq. (4), assuming a constant $T_e = 2.2$ eV (argon singly ionized) is e.g. less than 35 % at 50 ms after the first argon injection.

Fig. 4 summarises the comparison between the measured E_ϕ and E_c induced from argon and electron density measurements ($t = 1.05$ s) under different assumptions: argon density derived from spectroscopic measurements (spect); density increase after 1st argon puff all due to Ar⁺ (dne); argon density given by a homogeneous distribution in the torus of the injected argon (inj). Even assuming that neutral argon or ArIII (not yet measured) play a role in the RE slowing down, the friction force of the free and bound electrons is smaller than the electric force on the REs and can not account for the observed RE current decay.

Conclusions

The main finding of the described RE experiment is that the quantities of argon injected, to create and then suppress the REs, has a clear influence on the time decay of the RE beam, i.e. the more impurities, the faster the RE current decay. Nevertheless the critical electric field, calculated from the electron density and the concentration of singly ionized argon is 3-10 times lower than the toroidal electric field sustaining the RE beam, and cannot account for the RE current decay observed.

Acknowledgment. Michael Beck and Wolfgang Weisbart get the credit for maintaining and updating the AUG DMS. This work has been carried out within the framework of the EUROfusion Consortium and has received funding from the Euratom research and training programme 2014-2018 under grant agreement No 633053. The views and opinions expressed herein do not necessarily reflect those of the European Commission."



Left: fig. 3. Critical electric field, E_c (Eq. 3), as function of the Ar II density. A fully-ionized deuterium density of $2 \times 10^{19} \text{ m}^{-3}$ has been assumed in the background. The influence of neutral argon (Ar I) on E_c is also shown. Right: fig. 4. Critical electric field, E_c , calculated under different assumptions (see text), and E_ϕ (E_{exp}) deduced from U_{loop} measurements.